# REPORT DOCUMENTATION PAGE

AFRL-SR-BL-TR-99-

0089



| 1. AGENCY USE ONLY (*Leave Blank*) | 2. REPORT DATE | 3. REPORT TY |
|---|---|---|
| | May 1997 | Final (September 1996-February 1997) |

**4. TITLE AND SUBTITLE**
Multilayered Thermal Barrier Coatings by CVD

**5. FUNDING NUMBERS**
F49620-96-C-0049

**6. AUTHOR(S)**
Arthur J. Fortini, Sangvavann Heng, and Andrew J. Sherman

**7. PERFORMING ORGANIZATION NAME(S) AND ADDRESS(ES)**
Ultramet
12173 Montague Street
Pacoima, CA 91331

**8. PERFORMING ORGANIZATION REPORT NUMBER**
ULT/TR-97-7401

**9. SPONSORING/MONITORING AGENCY NAME(S) AND ADDRESS(ES)**
Department of the Air Force
Office of Scientific Research
Bolling AFB, DC 20332

**10. SPONSORING/MONITORING AGENCY REPORT NUMBER**

**11. SUPPLEMENTARY NOTES**
Small Business Innovation Research (SBIR) Program, Phase I; SBIR Rights Apply

**12a. DISTRIBUTION/AVAILABILITY STATEMENT**
Approved for public release; distribution unlimited.
SBIR Rights Apply

**12b. DISTRIBUTION CODE**

**13. ABSTRACT** (*Maximum 200 words*)
Turbine engine component life is currently limited by creep, creep-rupture, oxidation/corrosion, and thermomechanical fatigue. The use of protective coatings, such as nickel-chromium-aluminum-yttrium (NiCrAlY) and more recently platinum aluminides and various thermal barrier coatings (TBCs), has enabled higher temperatures and longer component life to be achieved, but component life and temperature capability still limit obtainable engine operating efficiency. Reduction in component temperature through the development and use of improved TBCs can dramatically extend component life, or conversely, allow higher operating temperatures to be used at constant component life. Additionally, lowering oxygen diffusion through the TBC will increase the life of the TBC itself, and reduce or eliminate oxidation and corrosion of the bondcoat and underlying component structure. Extension of TBC technology to increasingly complicated combustor, blade, and vane geometries and cooling passages requires improved application methods. In this project, Ultramet developed and demonstrated the chemical vapor deposition (CVD) of bondcoats and multilayered TBCs. Analytical modeling to quantify performance improvement predicted a 40-80°C drop in turbine blade temperature through the use of these coatings. In addition, burner rig oxidation and salt spray corrosion testing were performed on a coated blade.

**14. SUBJECT TERMS**
thermal barrier coating, chemical vapor deposition, turbine engine

**15. NUMBER OF PAGES**
24+Appendices

**16. PRICE CODE**

| 17. SECURITY CLASSIFICATION OF REPORT | 18. SECURITY CLASSIFICATION OF THIS PAGE | 19. SECURITY CLASSIFICATION OF ABSTRACT | 20. LIMITATION OF ABSTRACT |
|---|---|---|---|
| Unclassified | Unclassified | Unclassified | SAR |

# MULTILAYERED THERMAL BARRIER COATINGS BY CVD

Arthur J. Fortini, Sangvavann Heng, and Andrew J. Sherman
Ultramet
12173 Montague Street
Pacoima, CA 91331



May 1997

Final Report for Period September 1996 - February 1997





DEPARTMENT OF THE AIR FORCE
OFFICE OF SCIENTIFIC RESEARCH
BOLLING AFB, DC 20332

## TABLE OF CONTENTS

# LIST OF FIGURES

## GLOSSARY

| Term | Definition |
|---|---|
| AAS | atomic absorption spectroscopy |
| AFOSR | Air Force Office of Scientific Research |
| ASTM | American Society for the Testing of Materials |
| CVD | chemical vapor deposition |
| EB-PVD | electron beam physical vapor deposition |
| EDS | energy-dispersive X-ray spectroscopy |
| ICP | inductively coupled plasma |
| $lb_m$ | pounds mass |
| NiCrAlY | nickel-chromium-aluminum-yttrium |
| psia | pounds per square inch, atmospheric |
| PtAl | platinum aluminide |
| SBIR | Small Business Innovation Research |
| SEM | scanning electron microscopy |
| TBC | thermal barrier coating |
| tmhd | tetramethylheptanedionate |
| XRD | X-ray diffraction |
| $Y_2O_3$ | yttrium oxide (yttria) |
| YSZ | yttria-stabilized zirconia |
| $Y(tmhd)_3$ | yttrium tetramethylheptanedionate |
| $ZrO_2$ | zirconium oxide (zirconia) |
| $Zr(tmhd)_4$ | zirconium tetramethylheptanedionate |
| 1-D | one-dimensional |
| 3-D | three-dimensional |

# 1. INTRODUCTION

This is the final technical report submitted by Ultramet, Pacoima, CA 91331 to the Air Force Office of Scientific Research (AFOSR), Bolling AFB, DC 20332 under SBIR Phase I contract F49620-96-C-0049. The period of performance was from 1 September 1996 through 1 March 1997. The principal investigator was Andrew J. Sherman, supported by Sangvavann Heng and Arthur J. Fortini as project engineers. The AFOSR project manager was Alexander Pechenik.

Turbine engine component life is currently limited by creep, creep-rupture, oxidation/corrosion, and thermomechanical fatigue. The use of protective coatings, such as nickel-chromium-aluminum-yttrium (NiCrAlY) and more recently platinum aluminides and various thermal barrier coatings (TBCs), has enabled higher temperatures and longer component life to be achieved, but component life and temperature capability still limit obtainable engine operating efficiency. Reduction in component temperature through the development and use of improved TBCs can dramatically extend component life, or conversely, allow higher operating temperatures to be used at constant component life. Additionally, lowering oxygen diffusion through the TBC will increase the life of the TBC itself, and reduce or eliminate oxidation and corrosion of the bondcoat and underlying component structure. Extension of TBC technology to increasingly complicated combustor, blade, and vane geometries and cooling passages requires improved application methods. In this project, Ultramet developed and demonstrated the chemical vapor deposition (CVD) of bondcoats and multilayered TBCs. Analytical modeling to quantify performance improvement predicted a 40-80°C (72-144°F) drop in turbine blade temperature through the use of these coatings. In addition, burner rig oxidation and salt spray corrosion testing were performed on a coated blade.

## 2. BACKGROUND

The performance of turbine engines is limited by the maximum allowable use temperature of the hot section components, including interturbine ducts, combustor cans, stator vanes, and turbine blades. Current materials of construction are limited to an upper use temperature of approximately 1038°C (1900°F). To allow higher combustion temperatures to be used, engine components are currently cooled using compressor bleed air, decreasing engine performance. The upper use temperature of current materials is limited by their strength and life, such that a tradeoff is reached between cooling air requirements and material properties, maximum use temperature, environmental resistance, and life.

The development of advanced cooling schemes, protective coatings, and thermal barrier coatings (TBCs) has allowed ever-increasing turbine inlet temperatures to be achieved with acceptable component life and cooling requirements. However, due to increasingly complex cooling passages and greater turbine temperature and life requirements, current protective coating compositions and deposition/application technologies are inadequate for use in future turbine engines.

Several significant problems exist with state-of-the-art coating technologies, including platinum aluminide (PtAl) and nickel-chromium-aluminum-yttrium (NiCrAlY) bondcoats and yttria-stabilized zirconia (YSZ) thermal barrier coatings applied variously by pack cementation, electron beam physical vapor deposition (EB-PVD), low pressure plasma spraying, and atmospheric pressure plasma spraying. The specific weaknesses of current coatings to be overcome with the proposed technology investigated in the current work include the following:

- High oxygen permeability of current TBCs, leading to bondcoat and substrate (airfoil component) oxidative/corrosive degradation and failure [1-3].
- Low mechanical strength and resultant high thickness requirements for current TBC/bondcoat combinations, limiting applicability to rotating airfoil components.
- Fatigue debits caused by the application of brittle overcoatings and surface oxidation.
- Poor hot sulfur compatibility/corrosion resistance of current YSZ TBCs.
- Poor throwing power of current advanced coating technologies, preventing their uniform application to cooling channels and complex shapes.
- High cost and slow processing time of EB-PVD (which otherwise produces very high-quality advanced TBCs and is the present state of the art).

These weaknesses can be overcome through the use of innovative chemical vapor deposition (CVD) coating technology, use of alternate stabilizers, and reduction of the thermal conductivity and oxygen permeability of the coating by using sealcoat and multiple layer capabilities. Specifically, these current coating/component life limitations can be addressed as follows:

- <u>Bondcoat/substrate oxidation/corrosion</u>: Platinum bondcoats and multilayered TBCs incorporating platinum seal layers can be used to reduce TBC oxygen permeability. Based on relative oxygen diffusivities and estimated temperature gradients, the oxygen transport rate should be decreased by two to three orders of magnitude. This in turn would reduce or eliminate oxidative/corrosive attack of the bondcoat and substrate materials.
- <u>Limited mechanical strength</u>: The use of multilayered TBCs containing reflective layers, such as platinum, can provide a two- to three-fold decrease in radiative thermal transport, which is the dominant heat conduction mechanism at high temperatures. This in turn would reduce the coating thickness required, allowing application to high-speed rotating airfoil components.

- Fatigue debit: By allowing operation at lower temperatures, higher fatigue life is obtained in the airfoil component. Reduced contamination and embrittlement of the bondcoat and substrate materials will be achieved by reducing TBC oxygen permeability. The use of a platinum or platinum aluminide bondcoat would eliminate a brittle surface layer, and the use of CVD and sealcoat technologies would reduce the fatigue debit due to protective coating application. Further increase in fatigue life can be obtained by introducing residual surface compressive forces (e.g. through shot peening) or the application of a high fatigue strength ductile alloy surface coating (e.g. platinum) as part of the coating system.
- Poor hot corrosion resistance: Attack of current, primarily YSZ TBCs is caused mainly by preferential removal of the stabilizing element and accelerated crack extension of the substrate (stress corrosion cracking). While yttrium oxide and tantalum oxide stabilizers are much more stable against hot corrosion than their magnesium oxide or calcium oxide predecessors, stress corrosion cracking still occurs to a limited extent. Yttrium oxide also has a lower susceptibility to water and sulfur attack than the primary alternate stabilizer, cerium oxide. The use of platinum or platinum aluminide layers would dramatically reduce scale permeability and thus further protect the substrate from hot corrosion.
- Uniformity of application: The use of CVD for coating application would allow uniform coating of extremely complex shapes, including cooling holes and channels. CVD also offers the ability to grade the coating composition and produce dense coatings, potentially at a much higher rate (and hence lower cost) than state-of-the-art EB-PVD methods.
- Cost: CVD is potentially an order of magnitude faster than EB-PVD, and eliminates the need for highly refined, expensive targets for application. This would allow an estimated 80-90% reduction in the production cost of TBCs compared to EB-PVD.

This project demonstrated several technologies, including the ability to codeposit yttria and zirconia by CVD and the ability to deposit multilayered TBCs consisting of alternating layers of platinum and codeposited yttria and zirconia ($ZrO_2 \cdot Y_2O_3$). The use of a more oxidation- and corrosion-resistant platinum bondcoat, in addition to the standard NiCrAlY bondcoat, was investigated. Burner rig oxidation testing was performed to evaluate durability in a simulated turbine engine environment, and salt spray corrosion testing was performed to evaluate hot corrosion resistance.

## 3. EXPERIMENTAL APPROACH

### 3.1 Technical Objectives

The primary objectives of this project were to demonstrate, through analytical and experimental efforts, that a dramatic increase in airfoil life and temperature capability can be achieved at an acceptable cost by using chemical vapor deposition to fabricate multilayered thermal barrier coatings, and that significant advantages can be realized through the use of thin TBC coatings which can be applied to airfoils. To achieve these goals, the experimental approach was divided into three broad areas: mathematical modeling, CVD process development, and coating performance verification testing.

The series of multilayered coating systems illustrated in Figure 1 was investigated analytically and experimentally for further process development. They included current TBCs with sealcoats for increased life and new multilayered TBCs for increased temperature capability, lower oxygen permeability, and lower thermal conductivity.

Specific project objectives included:

- Development of physics-based models for prediction of airfoil temperature with and without TBCs. Based on this information, more detailed models could be developed in future work for predicting the oxygen transport rate through the various coating layers, and overall airfoil component life.
- Development of CVD processing parameters for codepositing controlled compositions in the $ZrO_2 \cdot Y_2O_3$ coating system.
- Development of CVD processing parameters for depositing platinum under temperature and pressure conditions similar to those used to deposit $ZrO_2 \cdot Y_2O_3$.
- Screening of platinum and NiCrAlY bondcoats with respect to coating adhesion and nucleation.
- Performance validation through burner rig oxidation and hot salt corrosion testing of representative coupons.

The goal of the project was to demonstrate that dramatic improvements can be made to thermal barrier and oxidation-protective coating systems by combining their respective functions into one multifunctional system, and that CVD is a viable processing route for the fabrication of these advanced coating systems. A key issue was demonstration of the application of sufficiently thin coatings to airfoils that would show sufficient advantage to justify their use.

A three-step technical approach was taken to meet the project objectives and provide guidance for further developments to be pursued in future work. The technical approach encompassed analytical modeling, process development, and performance validation.

### 3.2 Analytical Modeling

Analytical modeling was performed by NovaTech (Lynchburg, VA). This analysis consisted of two models: a simple one-dimensional (1-D) model and a three-dimensional (3-D) finite element model. Details of the NovaTech modeling effort are given in Appendix A.

In both models, the substrate alloy was assumed to be MAR-M 247, the gas temperature was 1500 K (2241°F), and the Reynolds number was $5 \times 10^5$. The TBC was assumed to comprise six layers of platinum (each 2 $\mu$m thick) alternating with five layers of yttria-stabilized zirconia (each 25 $\mu$m thick).

The goal of the first model was to predict trends and qualitatively assess the performance of the coating system. Because this model was one-dimensional, a closed-form analytical solution was possible. The 3-D finite element model, on the other hand, involved a more detailed approach. The 3-D model was also operated under two different sets of assumptions: one where the blade was assumed to be solid, and one where the blade was assumed to be hollow with cooling air on the interior.

### 3.3 Process Development

The goal of this portion of the project was to determine the process parameters for the deposition of $ZrO_2 \cdot Y_2O_3$ via a low temperature CVD process. While these oxides can be deposited via the traditional chloride processes (i.e., decomposition of the respective metal chlorides), the high temperatures required for that approach would damage or simply melt the alloy substrates. For this reason, a lower temperature, organometallic route was desired.

Initial attempts at depositing $Y_2O_3$ from yttrium ethylhexanoate were unsuccessful. As the temperature of the precursor bed was increased, it began decomposing before any appreciable vaporization took place. Zirconium ethylhexanoate behaved in a similar manner. While these precursors were comparatively inexpensive, they lacked sufficient vapor pressure to be used in a CVD process.

The next precursor to be used was zirconium tetramethylheptanedionate [$Zr(tmhd)_4$]. Using this precursor, a dense white deposit was obtained on the first CVD run. X-ray diffraction (XRD) analysis of the deposit showed it to be primarily tetragonal $ZrO_2$ with small amounts of the monoclinic phase. Use of the yttrium tetramethylheptanedionate [$Y(tmhd)_3$] precursor similarly resulted in a dense coating of $Y_2O_3$ on the first CVD run.

These initial coating runs were performed using graphite coupons as substrates. Once the precursors were downselected, various alloy substrates were then used. These included 321 stainless steel, Hastelloy-X, molybdenum, MAR-M 247, Inconel 617, and CMSX single-crystal superalloy. The deposition runs using these substrates focused on codepositing the $ZrO_2$ and $Y_2O_3$ materials in the desired proportions. As discussed below, codeposition of the two materials was achieved, but control of their relative proportions proved elusive.

The bondcoat investigation included uncoated substrates as well as specimens coated with plasma-sprayed NiCrAlY, oxidized NiCrAlY, and CVD platinum. The NiCrAlY-coated specimens were supplied by Williams International (Walled Lake, MI), while platinum CVD was performed by Ultramet. Because Ultramet has extensive experience in depositing platinum via CVD, very little development work was required. The CVD platinum was applied to both bare substrates and NiCrAlY-coated substrates.

### 3.4 Performance Validation

Based on the results of process development, a MAR-M 247 turbine blade with a plasma-sprayed coating of NiCrAlY was overcoated with CVD platinum. The part was then coated with alternating layers of $ZrO_2 \cdot Y_2O_3$ and platinum. A total of five platinum layers and four oxide layers were deposited. The outermost layer was a platinum sealcoat. The part was then sent to Williams International for burner rig oxidation testing and salt spray corrosion testing.

An identical part was coated with yttria-stabilized zirconia via the standard industrial EB-PVD process for use as a control specimen. Both parts were mounted side-by-side in the Williams burner rig for oxidation testing. Details of the Williams International test effort are given in Appendix B.

The burner rig oxidation testing was fueled with Jet-A, and the fuel/air ratio in the burner was approximately 0.044. The flow rate of air through the rig was $\approx 0.25\ lb_m/sec$ at 30 psia with ambient inlet air temperatures. The fuel flow was $\approx 30\ lb_m/hr$, but varied according to the burner operating temperature.

The first stage of the test comprised 13.1 hours of exposure at an operating temperature of 927°C (1700°F). After examining the parts, the test temperature was increased to 1010°C (1850°F), and the test was run for an additional 11.75 hours. Following the burner rig oxidation testing, the blades were removed and subjected to salt spray corrosion testing per ASTM B-117.

## 4. RESULTS AND DISCUSSION

### 4.1 Analytical Modeling

The goal of the first model was to predict trends and qualitatively assess the performance of the coating system. Because this model was one-dimensional, a closed-form analytical solution was possible. As shown in Figure 2, the thermal barrier coating dramatically decreased the temperature of the underlying blade. The maximum temperature drop predicted was 180°C (324°F), near the base. Closer to the blade tip, however, the effect of the coating on the blade temperature became insignificant.

In the 3-D finite element model, the temperature trends were similar to those predicted by the 1-D model, as shown in Figures 3 and 4. Once again, dramatic temperature reductions were observed near the base of the blade, and the effect became less pronounced near the tip.

A hollow blade with internal cooling air was also modeled in three dimensions using finite element analysis. In this case, the temperature profile from the base to the tip of the blade was quite flat. The most significant result was that the temperature drop due to the TBC was a uniform 40°C (72°F) over virtually the entire surface of the blade and through the entire thickness of the wall. This effectively predicts that the underlying alloy will be 40°C cooler at every location if the multilayered TBC is used. This is a very important result. Such a dramatic drop in temperature can be used either to increase the gas temperature and hence turbine efficiency, or to increase the useful life of the turbine components at current performance levels.

In all these calculations, the thermal conductivity of the multilayered coating was modeled as a monolayered coating with a bulk thermal conductivity based on the volume average of the platinum and $ZrO_2$ layers. In a more detailed model, the effects of the multilayered structure would be taken into account. This would include the effects of radiative heat transfer and the effectiveness of the platinum layers. Given a detailed steady-state temperature profile and the literature values for the diffusivity of oxygen in platinum and YSZ, the steady-state diffusive flux of oxygen can be determined. This in turn can be used to estimate the effective lifetime of the coated blade.

Complete results of the NovaTech modeling effort are given in Appendix A.

### 4.2 Process Development

As noted previously, control of the relative amounts of $ZrO_2$ and $Y_2O_3$ in the coating was extremely difficult. This was due primarily to the difficulty in determining the chemical composition of the coatings. The $Y_2O_3$ peak is not visible through XRD analysis, and when analyzed via energy-dispersive X-ray spectroscopy (EDS), the yttrium peak is obscured by the zirconium peak. As a result, the composition of the coating was estimated by knowledge of the deposition rates of the individual oxides under the conditions used, a crude estimate at best. A more reliable technique would involve digestion of the coating and chemical analysis of the resulting solution by atomic absorption spectroscopy (AAS) or inductively coupled plasma (ICP) analysis. However, time and funding limitations prevented such an analysis in this project.

Initially, it was discovered that the $ZrO_2 \cdot Y_2O_3$ coatings experienced very poor nucleation kinetics when applied to uncoated or NiCrAlY-coated substrates. The sparse nucleation resulted in the very porous and nodular coating shown in Figures 5A-B. However, when a CVD platinum bondcoat was used, much better nucleation occurred and a dense coating was obtained, as shown in Figures 6A-B. As can be seen, columnar growth was also achieved.

A total of 27 oxide deposition runs were performed. Based on these runs, it was found that the following conditions worked best:

- $Y(tmhd)_3$ bed temperature: 130-145°C (266-293°F)
- Argon flow to $Y(tmhd)_3$ bed: 50 $cm^3$/min
- $Zr(tmhd)_4$ bed temperature: 195-205°C (383-401°F)
- Argon flow to $Zr(tmhd)_4$ bed: 150 $cm^3$/min
- Oxygen flow rate: 10%
- Substrate temperature: 500-550°C (932-1022°F)
- Reactor pressure: 10-13 torr
- Bondcoat: plasma-sprayed NiCrAlY overcoated with CVD platinum

### 4.3 Performance Validation

Two turbine blades were subjected to burner rig oxidation testing at Williams International: the Ultramet coated blade with multiple layers of platinum and $ZrO_2 \cdot Y_2O_3$, and a control specimen coated with a single layer of YSZ by EB-PVD. The first segment of the test comprised 13.1 hours at an operating temperature of 927°C (1700°F). Neither of the test articles showed any signs of cracking or spallation, as shown in Figure 7. The temperature was then increased to 1010°C (1850°F) and the test run for an additional 11.75 hours. After this second segment of the testing, some cracking was observed near the tip of the Ultramet coated blade, as shown in Figure 8. The control specimen showed no degradation. Despite the cracking observed after the 1850°F testing, the Ultramet coating remained well-adhered to the substrate; no spallation occurred.

The blades were then removed from the burner rig and subjected to salt spray corrosion testing per ASTM B-117. As shown in Figure 9, the Ultramet coated blade suffered corrosive attack, while the control specimen did not. EDS analysis of the green corrosion residue revealed high concentrations of nickel, oxygen, and chlorine. Small amounts of aluminum, cobalt, and sodium were also detected.

Because the cracking occurred only after the parts were heated above the phase transition temperature for unstabilized $ZrO_2$ (≈1000°C, or 1832°F), it is reasonable to assume that the coating did not contain sufficient $Y_2O_3$ to stabilize it. Given the difficulties encountered in measuring and estimating the exact coating composition of the $ZrO_2 \cdot Y_2O_3$ material, this is the most likely scenario.

Complete results of the Williams International test effort are given in Appendix B.

## 5. CONCLUSIONS AND RECOMMENDATIONS

### 5.1 Analytical Modeling

A more detailed model should be developed that accounts for the multilayered structure of the TBC. This would enable the model to quantify the effectiveness of the platinum layers at reducing radiative heating of the part. The resulting steady-state temperature profile could then be used in conjunction with literature values for oxygen diffusivity in platinum and YSZ to determine the steady-state oxygen flux through the coating, which in turn could be used to predict the lifetime of the coated part. A similar calculation for an EB-PVD coated part could be used to "calibrate" the analysis.

### 5.2 Process Development

The exact compositions of the $ZrO_2 \cdot Y_2O_3$ coatings deposited in this project were unknown. In future work, a quantitative means of determining the exact composition of the coating must be employed. AAS or ICP analysis of witness coupons would easily meet these requirements. The ability to accurately measure the coating composition would enable the process conditions for depositing the desired oxide composition, $ZrO_2$:$15Y_2O_3$, to be determined. This determination should require only minor modifications to the previously selected processing conditions.

The next step in process development would be to modify the CVD reactor so that both coatings, YSZ and platinum, can be applied without removal of the part. While depositing the multiple layers one at a time is satisfactory for initial development work, it is unsuitable for commercial-scale production. Initial plans for such a reactor have already been formulated.

Only a very narrow processing band and selection of precursors was pursued in this effort. Investigation of alternate precursors such as the ethoxides and other organometallics should be pursued in future work, as well as more detailed work in the halide systems, along with the development of processing-microstructure-properties relationships. Grain size, stabilizer content, porosity, texture, and deposition rate should be investigated in small-scale reactors leading to optimized TBC kinetics and structure.

### 5.3 Performance Validation

Once a process for depositing the desired coating composition is determined, the burner rig oxidation testing and salt spray corrosion testing must be repeated. Survival of coated parts in these tests in an unqualified manner is a necessary precondition for demonstrating the commercial viability of the multilayered TBC concept.

### 5.4 Cost

The final hurdle to development of a viable multilayered TBC is cost. Although the tetramethylheptanedionate (tmhd) precursors yielded the best coating performance, they are quite expensive. In order to reduce the overall cost of the coating process to a level where it becomes commercially viable, a less expensive source of the material is required.

A review of the literature suggests that each of the tmhd precursors can be synthesized from neat tmhd and a simple salt of the metal to be deposited. Assuming a 95% yield in the synthesis, the cost of the precursors can be reduced by almost 90%. Assuming 50% efficiency in the CVD process, the overall coating cost per square inch of substrate is estimated to be \$8.60. This cost includes not only the cost of the $Zr(tmhd)_4$ precursor, but also the cost of the $Y(tmhd)_3$ and platinum acetylacetonate precursors. Based on discussions with industry personnel, this cost is well within the realm of commercial feasibility.

Furthermore, because CVD is not a "line-of-sight" process (i.e., deposition occurs on all areas of a part regardless of its orientation within the CVD reactor), several hundred parts can be coated simultaneously in a single reactor. The net result will be a further decrease in the overall cost of the coating process.

Finally, the capital cost of CVD equipment is more than an order of magnitude less than a comparable EB-PVD system. Whereas an EB-PVD system will cost well over a million dollars, a CVD reactor and all of its associated components will cost less than \$100,000. Additionally, the corresponding CVD reactor would be larger and capable of handling a much greater number of parts. The resulting cost per part would therefore decrease even further.

## REFERENCES


1. C.C. Berndt, *Thin Solid Films* **108** (1983), 1.
2. E.Y. Lee, R.R. Biederman, and R.D. Sisson Jr., *Plasma Surface Engineering* **1** (1989), 365.
3. E.Y. Lee and R.D. Sisson Jr., *Proc. 7th Natl. Thermal Spray Conf.* (1994), 55.

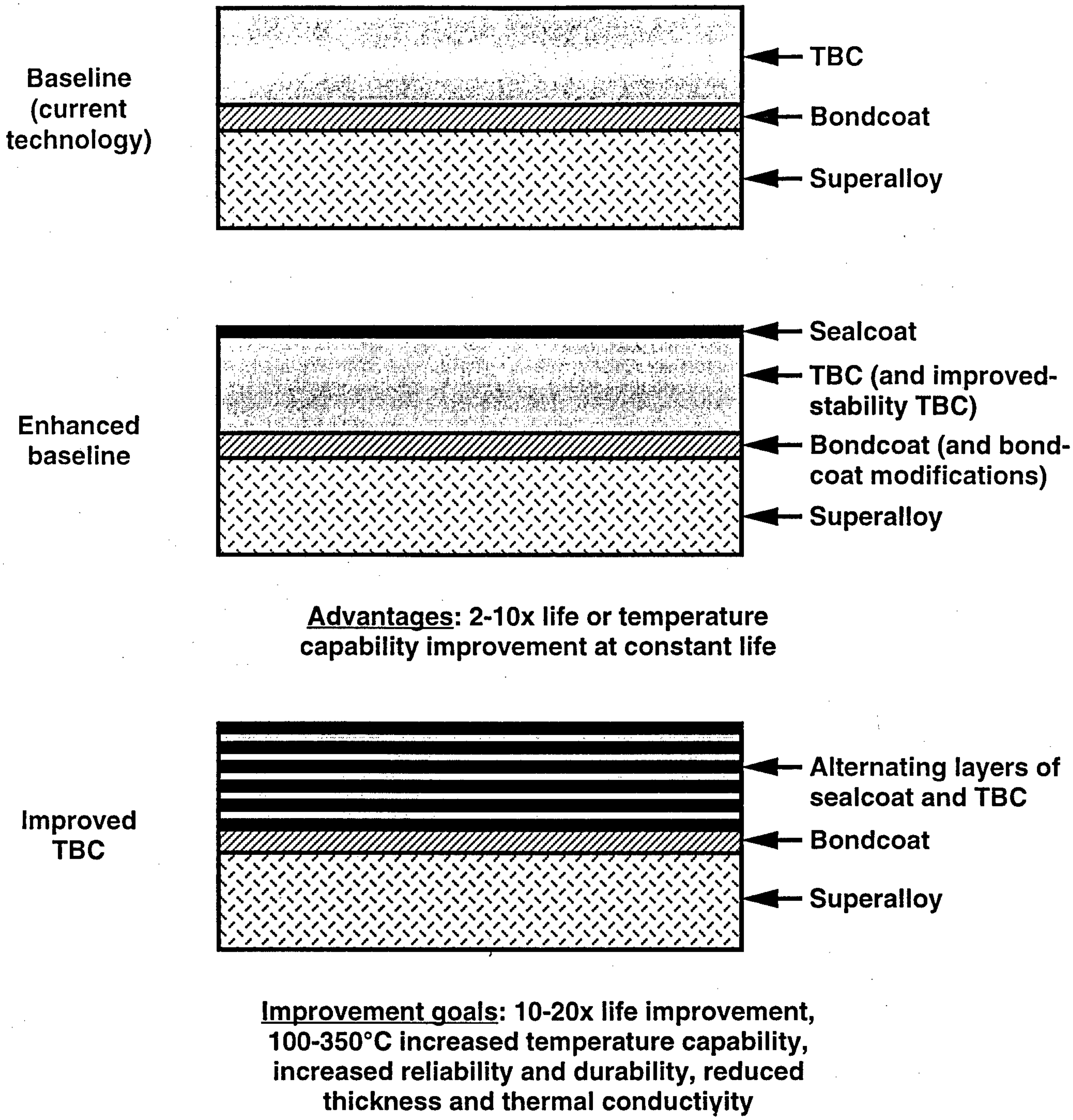


**Figure 1.**
Schematic of thermal barrier coating concepts

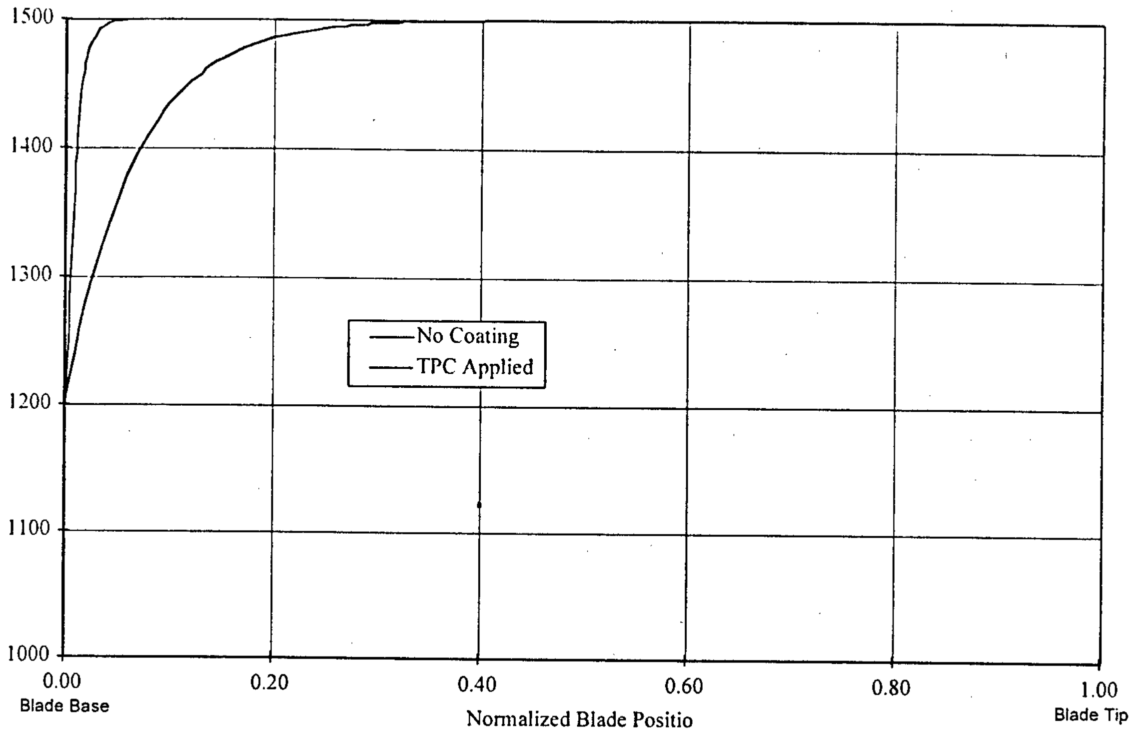


**Figure 2.**
Centerline temperature profiles predicted by 1-D model for uncoated and YSZ/platinum-coated turbine blades

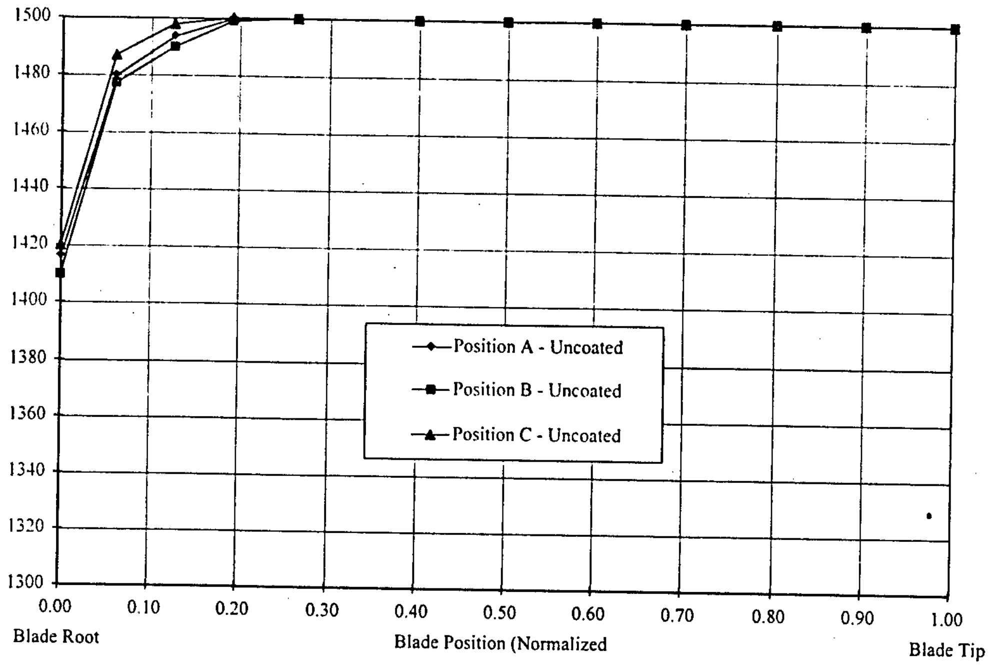


**Figure 3.**
Centerline temperature profiles predicted by 3-D model for passively cooled, uncoated turbine blades

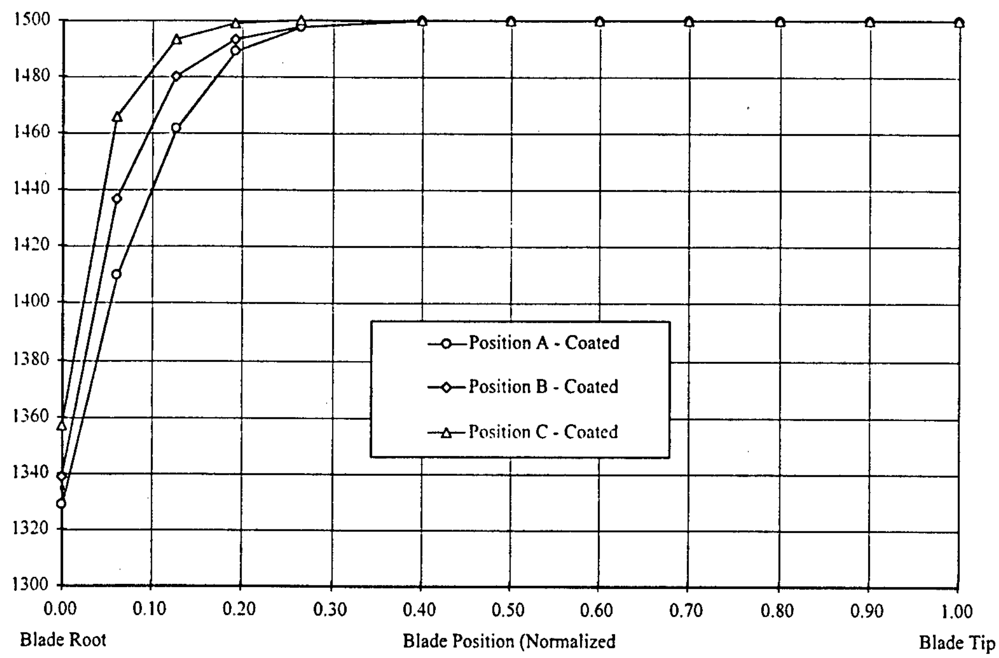


**Figure 4.**
Centerline temperature profiles predicted by 3-D model for passively cooled, YSZ/platinum-coated turbine blades

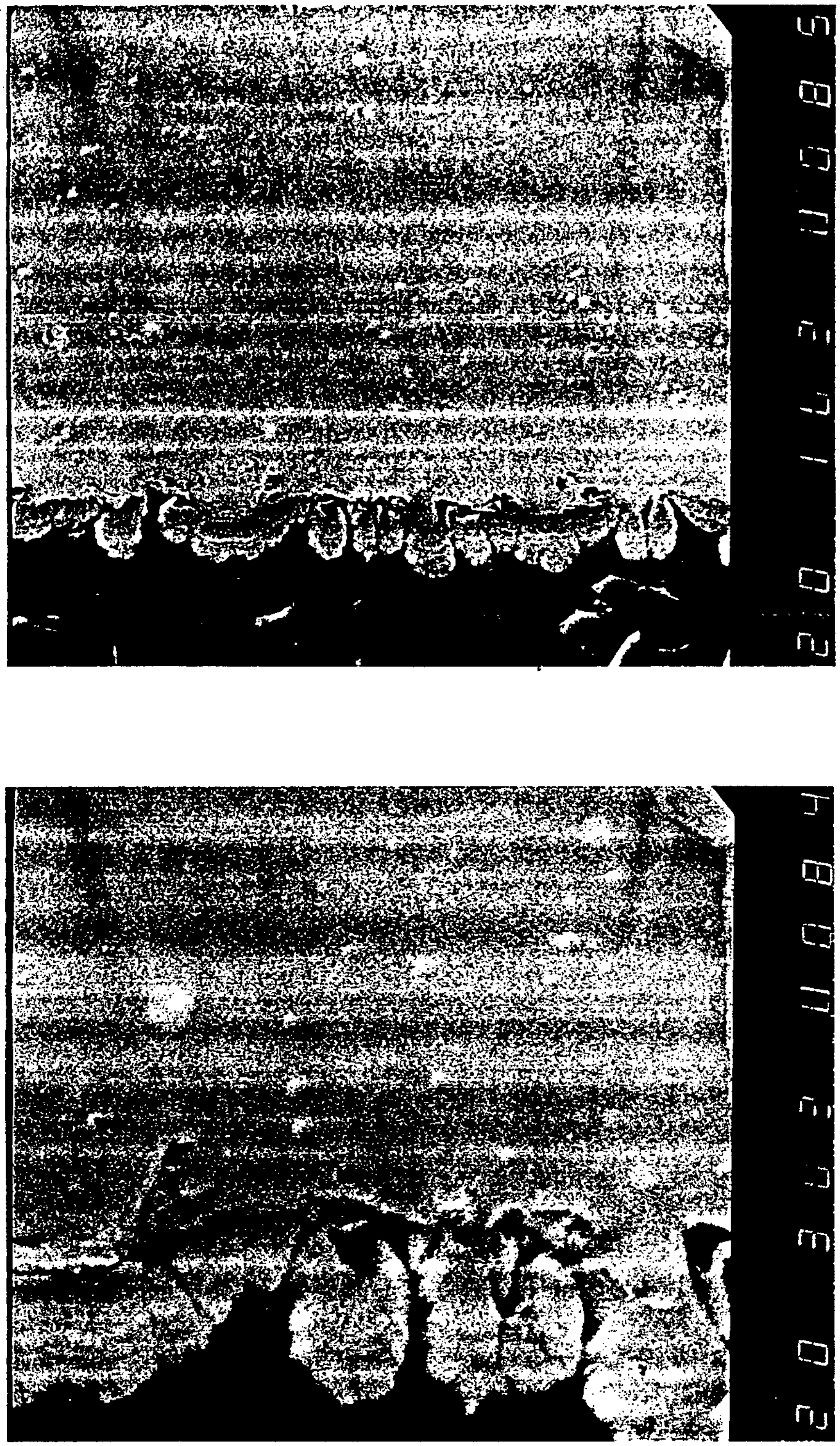

**Figures 5A-B.**

SEM micrographs (cross-section) of $ZrO_2 \cdot Y_2O_3$ codeposited on as-received MAR-M 247 substrate with no platinum interlayer, showing porous, nodular coating with poor adhesion (top: 1000×; bottom: 3000×)

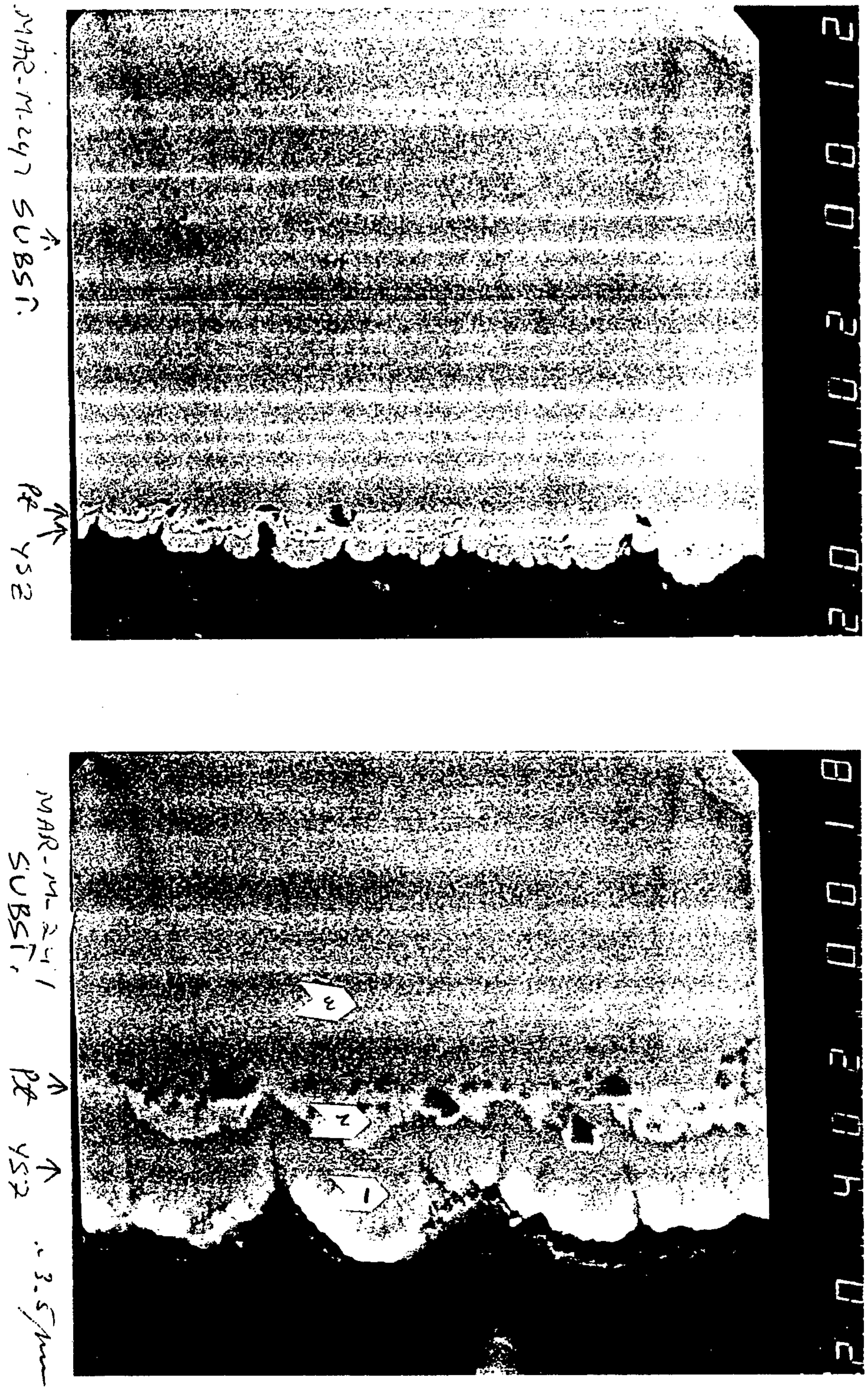


**Figures 6A-B.**
SEM micrographs (cross-section) of $ZrO_2 \cdot Y_2O_3$ codeposited on MAR-M 247 substrate with platinum interlayer, showing dense, columnar coating with good adhesion (top: 1000×; bottom: 4000×)

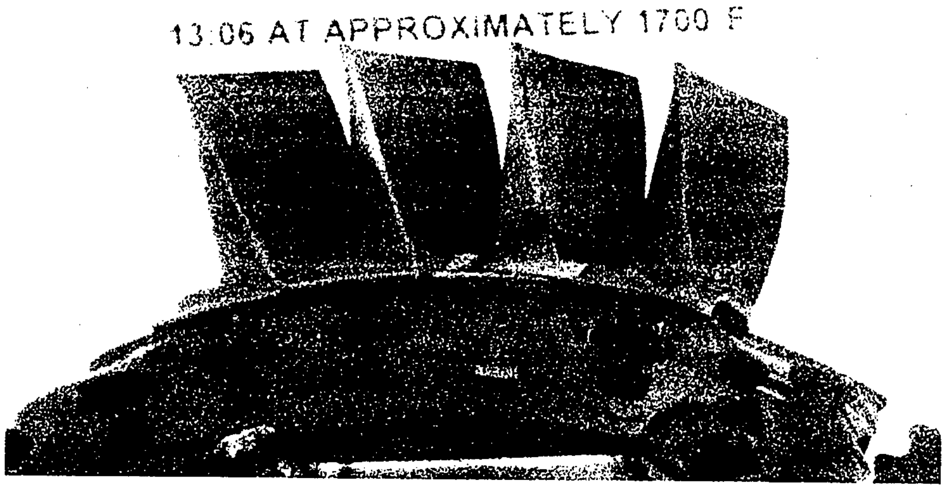


**Figure 7.**
Turbine blade test specimens after 13.1 hours of burner rig exposure at 1700°F, showing lack of cracking (Ultramet $ZrO_2 \cdot Y_2O_3$/platinum-coated blade is second from right)

**Figure 8.**

Turbine blade test specimens after 13.1 hours of burner rig exposure at 1700°F and 11.75 hours at 1850°F, showing cracking of Ultramet $ZrO_2 \cdot Y_2O_3$/platinum-coated blade (at right)

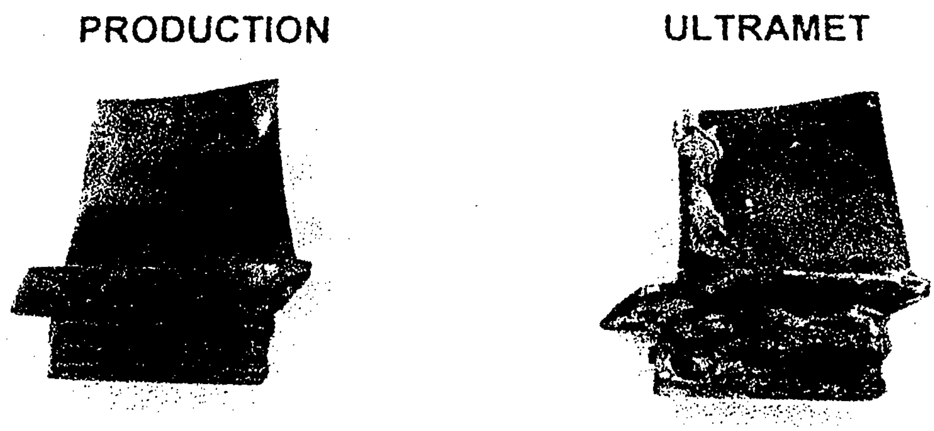


**Figure 9.**
Turbine blade test specimens after salt spray corrosion testing per ASTM B-117, showing corrosion of Ultramet $ZrO_2 \cdot Y_2O_3$/platinum-coated blade (at right)

## APPENDIX A.

NovaTech Data Package
for Analytical Modeling
of Multilayered Thermal Barrier Coating Performance

# 1. PURPOSE

Analyses were performed to assess the benefits of a multi-layered thermal barrier coating (TBC) on the thermal performance of passively cooled turbine blades under a Phase 1 Small Business Innovative Research (SBIR) program at Ultramet. These analyses were then extended to a representative cooled turbine blade to determine the effects of the TBC on actively cooled turbine blades.

A one dimensional analytical solution for the passively cooled blade were developed as a scoping tool to determine nominal heat transfer characteristics of the turbine blade as well as the temperature profiles of the blade from root to tip. The baseline design was then modeled numerically in three dimensional space to confirm the 1-D analyses and provide a reference point for the subsequent actively cooled models. Both the analytical and numerical models were based on the design provided by Williams International (Drawing #50344). To simplify the analysis, a uniform cross-section was assumed which did not include any blade twist. The analysis was further simplified by ignoring any variation in the heat transfer along the blade from the leading edge to the trailing edge. In each case, an average heat transfer coefficient was calculated and applied over the entire blade surface. Figure 1 is sketch of the blade used in this analysis. Since no design data for a specific actively cooled turbine blade was available, the passively cooled model was modified to include a generic internal cooling design.

# 2. ANALYSIS RESULTS

## 2.1 One-Dimensional Scoping Calculations

Scoping calculations were performed on the passively cooled turbine blade with and without the thermal protective barriers to determine the degree to which a TPB could reduce the overall blade temperature.

The 1-D model treats the blade as a uniform cross-section, extended surface attached to the turbine hub. Hence the only parameters of interest are the heat transfer to the blade from the free stream gas and conduction along the blade toward the blade root. Calculation of the heat transfer coefficient proceeds directly from standard boundary layer heat transfer for flat plates in a free stream[1,2]. For turbulent flow conditions, the average heat transfer coefficient is given by:

$$\bar{h} = \frac{Nu k}{L} = 0.0296 \, Re_L^{4/5} \, Pr^{1/3} \frac{k_G}{L} \, , \tag{1}$$

where L is the blade centerline length and $k_G$ is the thermal conductivity of the free stream gas. Hill and Peterson present experimental data for a number of small high pressure rotor blades which shows that $Re_L$ is in the range of $2 \times 10^5$ to $9 \times 10^5$. For this exercise, an average $Re_L$ value of $5 \times 10^5$ was used.

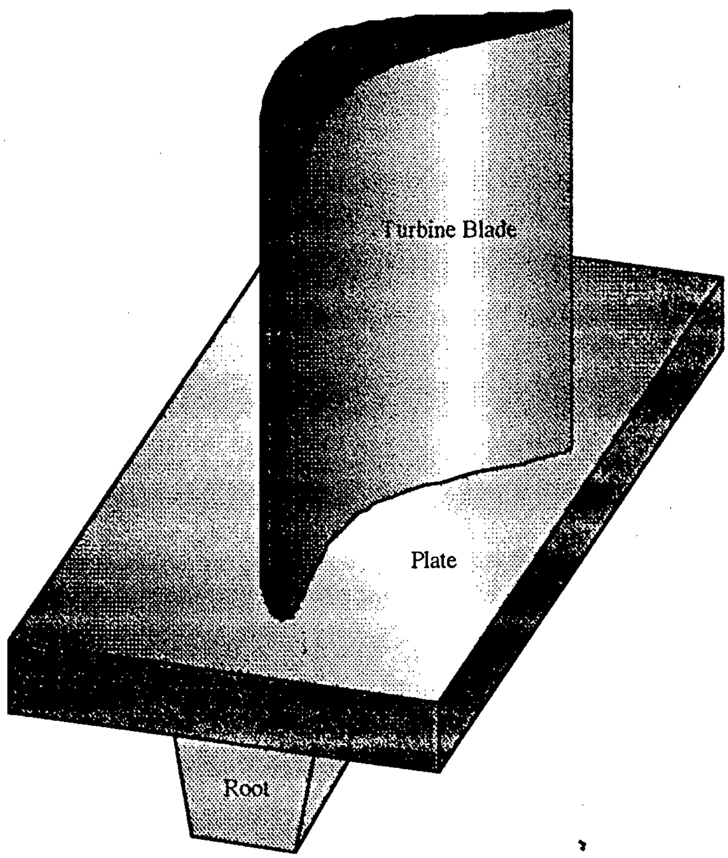


**Figure 1. Sketch of Turbine Blade.**

[1] Hill and Peterson, "*Mechanics and Thermodynamics of Propulsion, 2nd Edition*," Addison-Wesley, 1992.
[2] Incropera and DeWitt, "*Fundamentals of Heat and Mass Transfer, 3rd Edition*," Wiley and Sons, 1990.

Given a heat transfer coefficient, application of the general form of the steady-state energy equation for a 1-D extended surface yields a solution of the form:

$$\frac{d^2T}{dx^2} - \frac{hP}{kA_c}(T - T_\infty) = 0, \qquad (2)$$

in which k is the thermal conductivity of the blade (MAR-M 247 Alloy), P is the blade perimeter, and $A_c$ is the blade cross sectional area. Through a transformation of variables, Eq. 2 becomes,

$$\frac{d^2\theta}{dx^2} - m^2\theta = 0 \qquad (3)$$

where

$$\theta(x) \equiv T(x) - T_\infty, \ and$$

$$m^2 \equiv \frac{hP}{kA_c}.$$

With no TPB, the blade is essentially at the same temperature as the free stream gas except for very near the base of the blade where it intersects with the support plate as shown in Figure 2. In this region, high thermal gradients are present which will result in high thermally induced stresses.

It should be noted that in this simple model, the sink temperature is applied at the base of the blade whereas typically, this sink temperature is more closely associated with the blade root which will raise the magnitude of the temperature at the base of the blade but not significantly affect the profile.

Addition of a multi-layer TPB consisting of six layers of platinum (2 micron thickness) alternating with five layers of stabilized zirconia (25 micron thickness) resulted in significantly reduced temperatures (Figure 2) near the base of the blade while the top half of the blade remains essentially unchanged. It is quite possible that these reduced temperatures near the blade root are significant enough to reduce the thermal stresses in this region sufficiently to meet performance requirements.

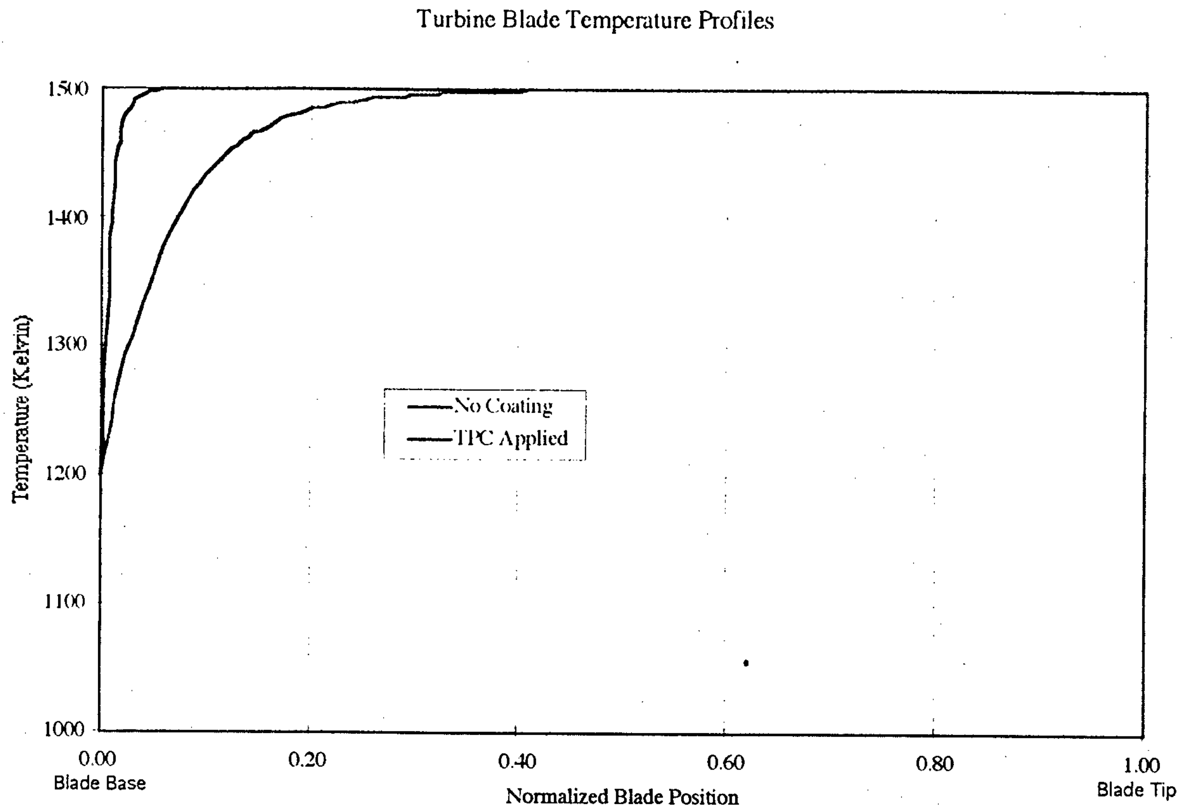


**Figure 2. Predicted Blade Temperature Profiles From One-Dimensional Model.**

## 2.2 Numerical Model of Passively Cooled Turbine Blade

Because of the simplifying assumptions made in the scoping calculations, a fully three-dimensional finite element model was generated using the SDRC I-DEAS/TMG software package and solved for the same conditions as the 1-D analysis. Figure 3 shows the finite element model used in this analysis. The blade measures 0.968-in along its chord with a height of 0.965-in. as measured from the intersection of the blade with the baseplate to the blade tip. The thickness was held constant along its height at 0.175-in. which is essentially the blade root thickness. The baseplate and blade root were modeled as solid blocks of approximately the right volume and dimensions.

In this analysis, the sink temperature was held constant in the root where it more closely approximates the real operating conditions and the baseplate was allowed to rise in temperature under adiabatic boundary conditions resulting from its geometry. The free stream gas was modeled at a temperature of 1500 Kelvin and convectively coupled to the blade using the heat transfer coefficient given by Eq. 1. This value of $h$ was applied uniformly over the surface of the blade. Two cases were run, one without and one with the TBC applied. In the case in which the TBC was applied, the coating was modeled as a single surface coating with a bulk thermal conductivity based upon the volume average of the platinum and zirconia layers. Hence no thermal gradients through the individual coating layers were obtained. Material properties for Mar-M 247 alloy were taken from the data supplied by Williams International to Ultramet[3] while the properties of both platinum and zirconia were taken from the literature.

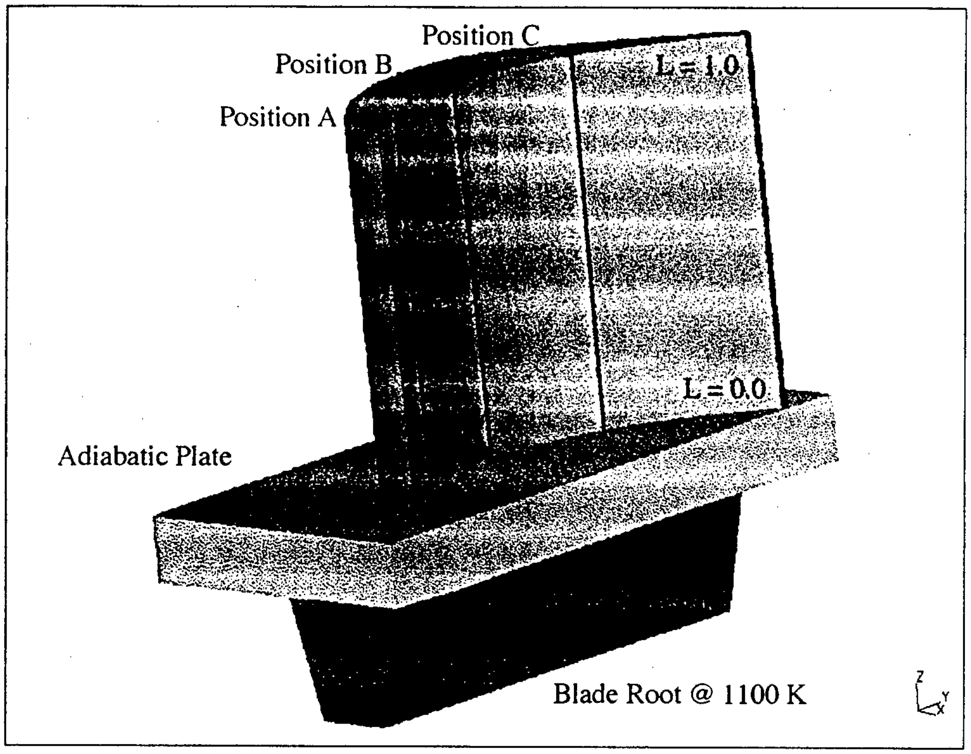


**Figure 3. Shaded Finite Element Model of Passively Cooled Turbine Blade.**

The numerical results matched closely to the 1-D calculation in terms of temperature profiles. Figures 4 and 5 are plots of the blade temperatures versus position along its length for selected locations (A, B, & C as indicated in Figure 3) along the blade centerline for both the uncoated and coated models. As can be seen, the TBC does significantly reduce the blade temperatures in the region near the baseplate as compared to the uncoated blade and should result in lower thermal stresses.

[3] William Fohey, Williams International, Letter to Vann Heng, Ultramet, July 10, 1997.

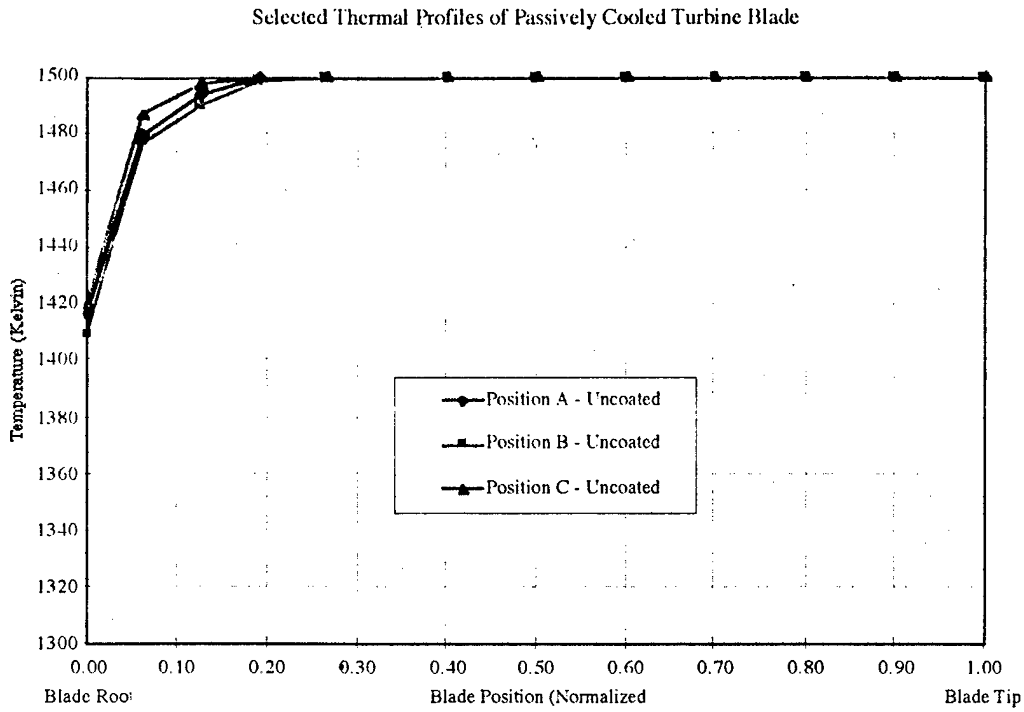


**Figure 4. Centerline Temperature Profiles of Passively Cooled, Uncoated Turbine Blade.**

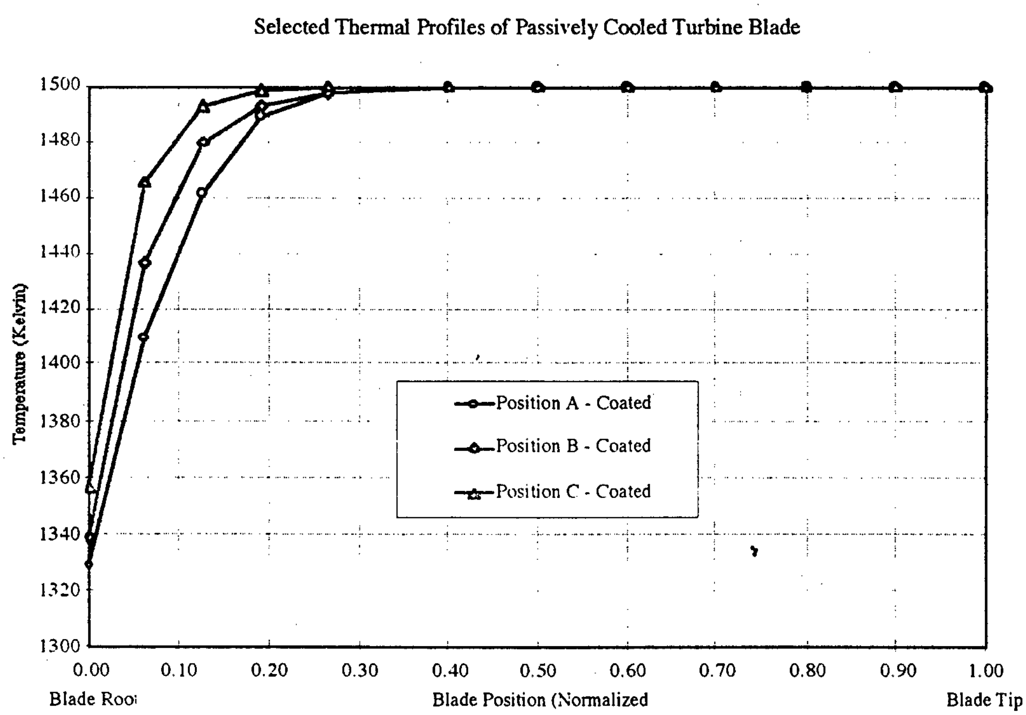


**Figure 5. Centerline Temperature Profiles of Passively Cooled, TBC Coated Turbine Blade.**

## 2.3 Numerical Model of Internally Cooled Turbine Blade

Typically, high temperature turbine blades are cooled by injecting a portion of the airflow from the compressor into the center of the blade where it is ducted through a number of passages before being exhausted through numerous small holes in the surface of the turbine blade itself. Using this method, the combined effects of cooling flow inside the blade and the presence of a cooled film on the surface can reduce the blade temperature by 200-300 Kelvin. To simulate this effect as nearly as possible, the previous model was modified to include a central single coolant passage. No exhaust flow holes on the surface of the blade were included as this was beyond the scope of this analysis. Instead, the internal flow was held at a constant temperature of 850 Kelvin and convectively coupled to the internal surface of the blade using an effective heat transfer coefficient calculated from published data on film cooled turbine blades (Hill and Peterson) which accounts for both the internal cooling and film cooling effects. Depending on the percentage of bypass flow from the compressor, (from 4-10% of the total flow through the compressor), the calculated heat transfer coefficients were on the order of 10 kW/m$^2$-K. Figure 6 shows a cutaway view of the finite element model used.

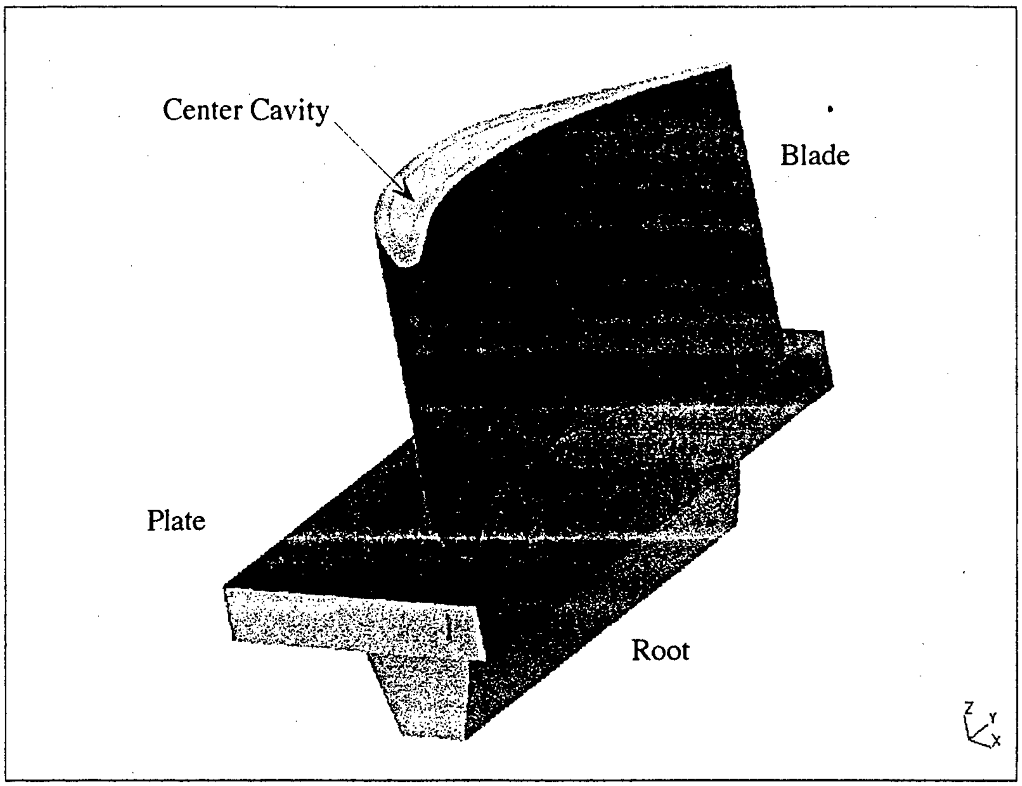


**Figure 6. Modified Turbine Blade Finite Element Model.**

As before, the model was solved for the case in which no coating was applied and for the case which included the multilayered TBC. Given the relatively good coupling to the internal cooling passage, the blade temperatures did not vary significantly from root to tip as before. Rather, the temperature contours varied through the thickness of the blade wall as expected. Figure 7 shows the outside surface temperature contours for the coated turbine blade while Figure 8 is a plot of the temperature contours through the blade wall midway along its height. In the location of the center cavity we see that the blade wall temperature is reduced by approximately 40 Kelvin from the uncoated blade.

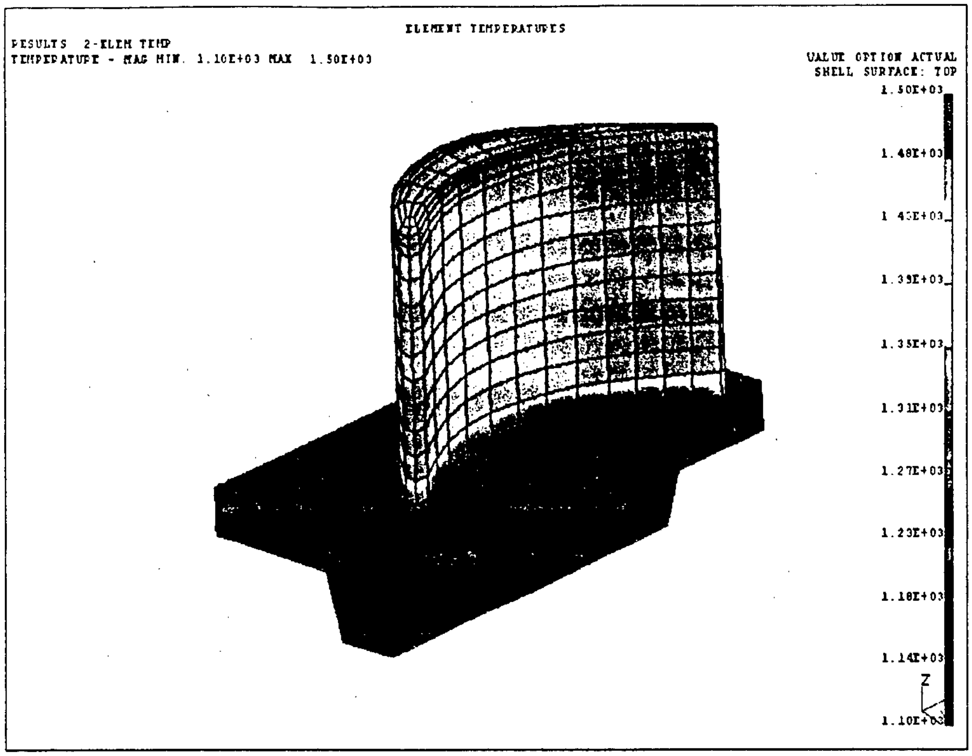


**Figure 7. Blade Surface Temperature Contours.**

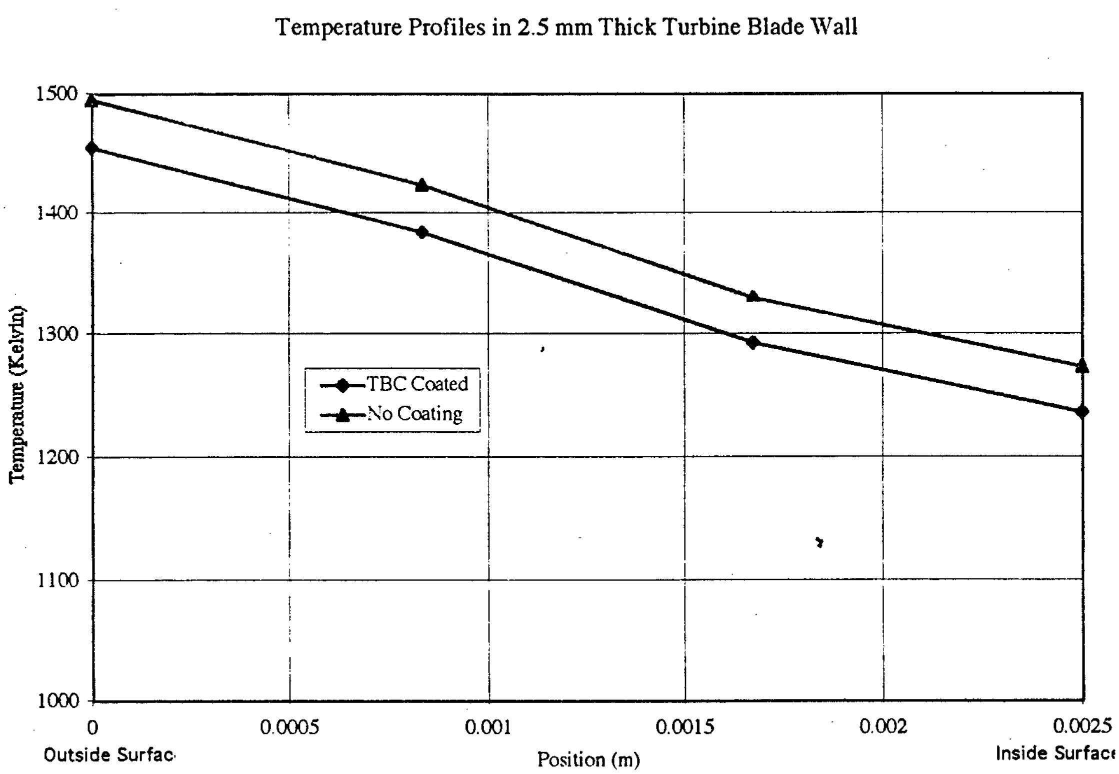


**Figure 8. Temperature Profile Through Wall of Cooled Turbine Blade.**

## 3. CONCLUSIONS AND RECOMMENDATIONS

Addition of a thermal barrier coating to representative turbine blades is found to significantly reduce the blade temperatures over that of uncoated blades. In the case of passively cooled blades, this effect is most observable at the blade root where stresses are highest. Similar results are found for a simple actively cooled turbine blade where overall blade temperatures are reduced by the addition of the TBC. Detailed thermal and thermohydraulic analyses on specific turbine blades, particularly those that are actively cooled, are needed to fully assess the benefits of the TBC from the standpoint of heat transfer. In addition, thermal stress analyses are needed based upon these results to determine whether the improved temperature profiles result in real gains in the mechanical performance of the turbine blade.

# APPENDIX B.

Williams International Data Package
for Burner Rig Oxidation and Salt Spray Corrosion Testing
of Multilayered Thermal Barrier Coatings

## Abstract

A multi-layered thermal barrier coating supplied by Ultramet was successfully applied to a Williams International high pressure turbine blade. In a side-by-side comparison, the Ultramet coating was compared to the production coating during burner rig and salt spray corrosion testing. The Ultramet coating survived intact up to 1700°F, but started to crack around 1850°F. Subsequent exposure of the same blades to salt spray corrosion testing resulted in significant corrosion deposits on the Ultramet coated blade but not on the production blade. It should be noted that the test articles were exposed to temperatures significantly higher than normal during burner rig operation.

## Procedure

Standard production coated (pack aluminide) HP turbine blades were supplied to Ultramet for coating. A multi-layered, platinum-zirconia coating was chemical vapor deposited. The Ultramet coated blade and one production coated blade were fixtured in a section of a turbine disk with thermocouples on the backside (downstream) side of the test articles. Another blade was placed on either side of the test articles to more closely approximate reflective effects (ref. Figs. 1 & 2). The fixture was positioned on the burner rig to achieve equivalent surface temperatures during operation (ref. Fig. 3).

Initial testing started at 1700°F for 13.1 hours (ref. Figs. 4 & 5). After visual inspection at several times, the surface temperature was increased to 1850°F for 11.75 continuous hours. Burner rig testing was terminated due to observed cracking on the Ultramet coating (ref. Figs. 6 & 7). Total burner rig exposure was 24.85 hours.

The test articles were subsequently exposed to 150 hours of salt spray corrosion testing per ASTM B-117. The blades were inverted and suspended by the blade dovetails for the duration of the test. An emerald-green residue was observed along with white salty residue on the Ultramet blade. No significant corrosion was observed on the production coating (ref. Fig. 8). Energy Dispersive Spectroscopy of the residue revealed high levels of nickel, oxygen, and chlorine (ref. Fig. 9). Aluminum, cobalt, and sodium were also detected. Although zirconium and platinum could have been present since they are coating constituents, zirconium, platinum, and phosphorus have overlapping peaks and could not be accurately distinguished.

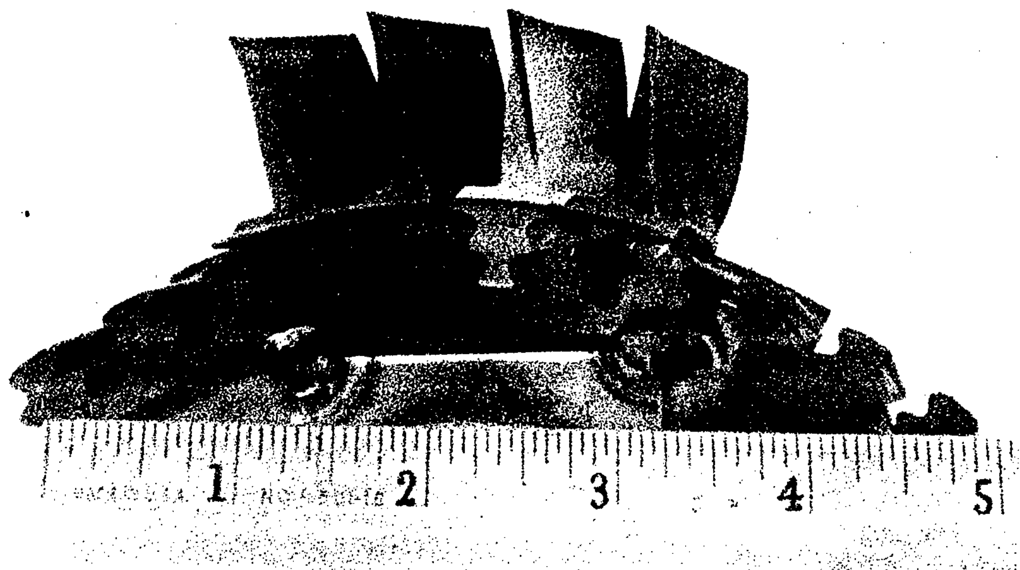

Figure 1. Test blades in disk fixture. Ultramet coating is on the second blade from the right.

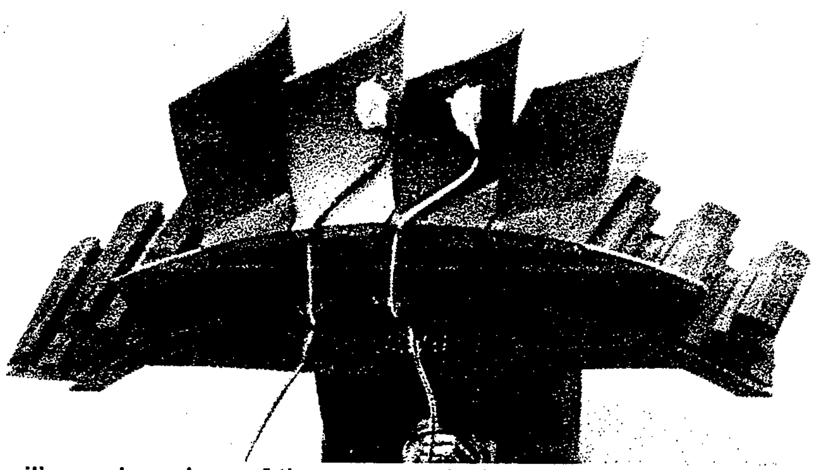

Figure 2. Trailing edge view of thermocoupled test blades. Ultramet coating is on the second blade from the left.

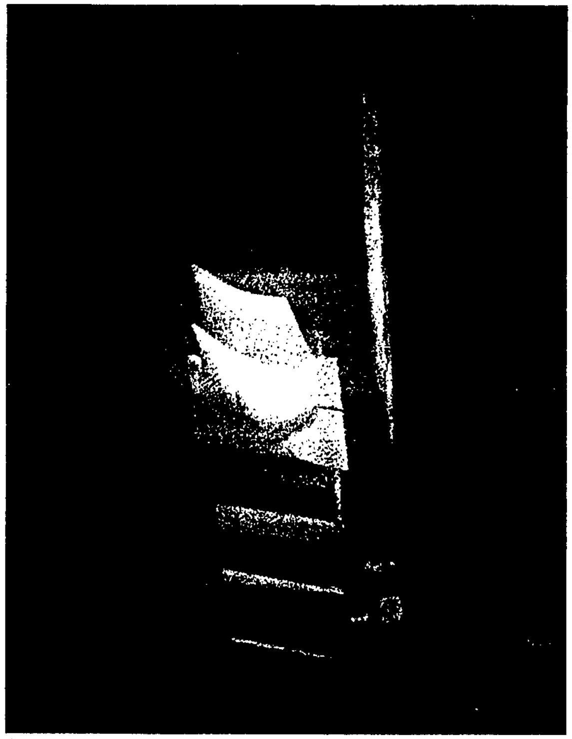

Figure 3. Two test blades used during setup of the burner rig. Thermocouples were placed on the same surfaces.

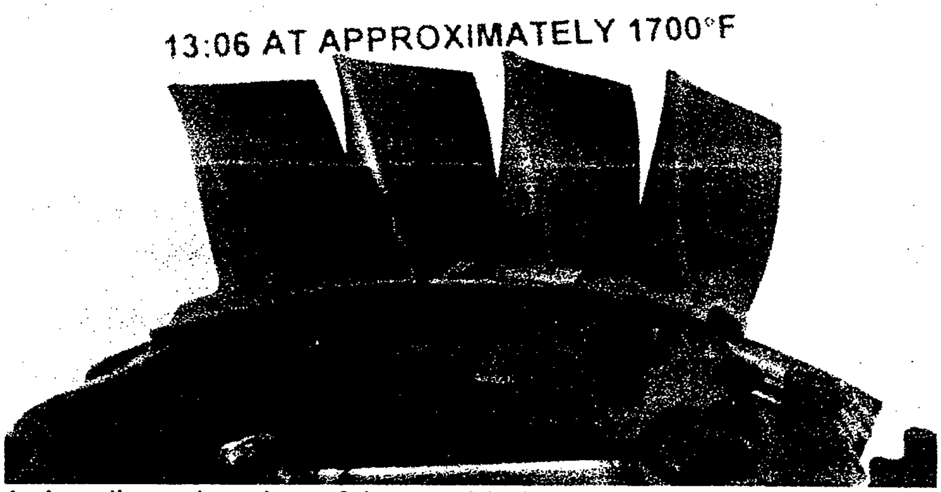


Figure 4. Leading edge view of the test blades after 13.1 hours of burner rig exposure at 1700°F. Ultramet coating is on the second blade from the right.

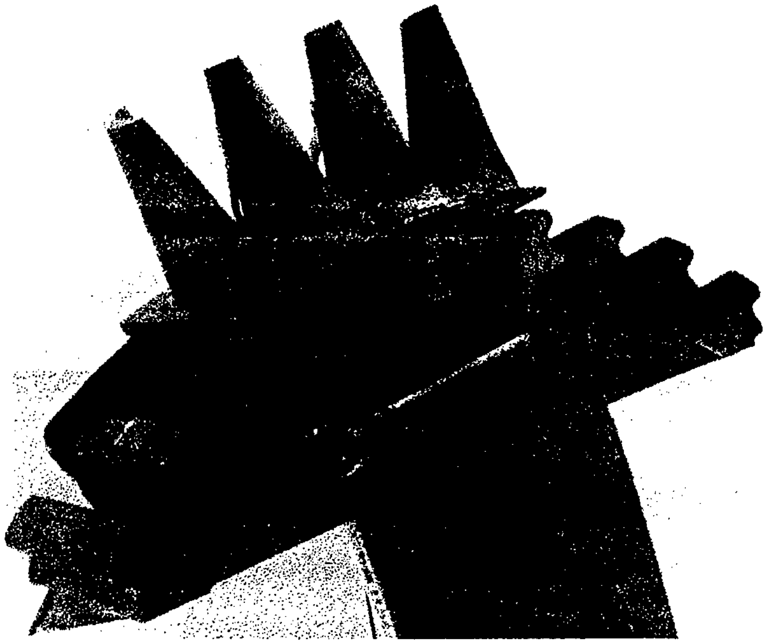

Figure 5. Leading edge view of same blades showing slight thermocouple disbond on the Ultramet coating.

ULTRAMET PRODUCTION

Figure 6. Test blades after 13.1 hours at 1700°F and 11.75 hours at 1850°F.

Figure 7. Test blades after 13.1 hours at 1700°F and 11.75 hours at 1850°F. Note cracking in the Ultramet coating on the right.

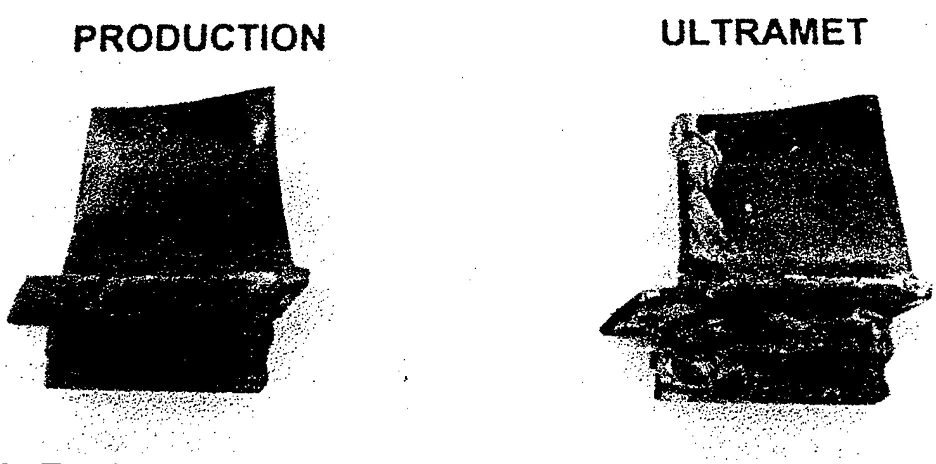


Figure 8. Test blades after 150 hours of salt spray testing.

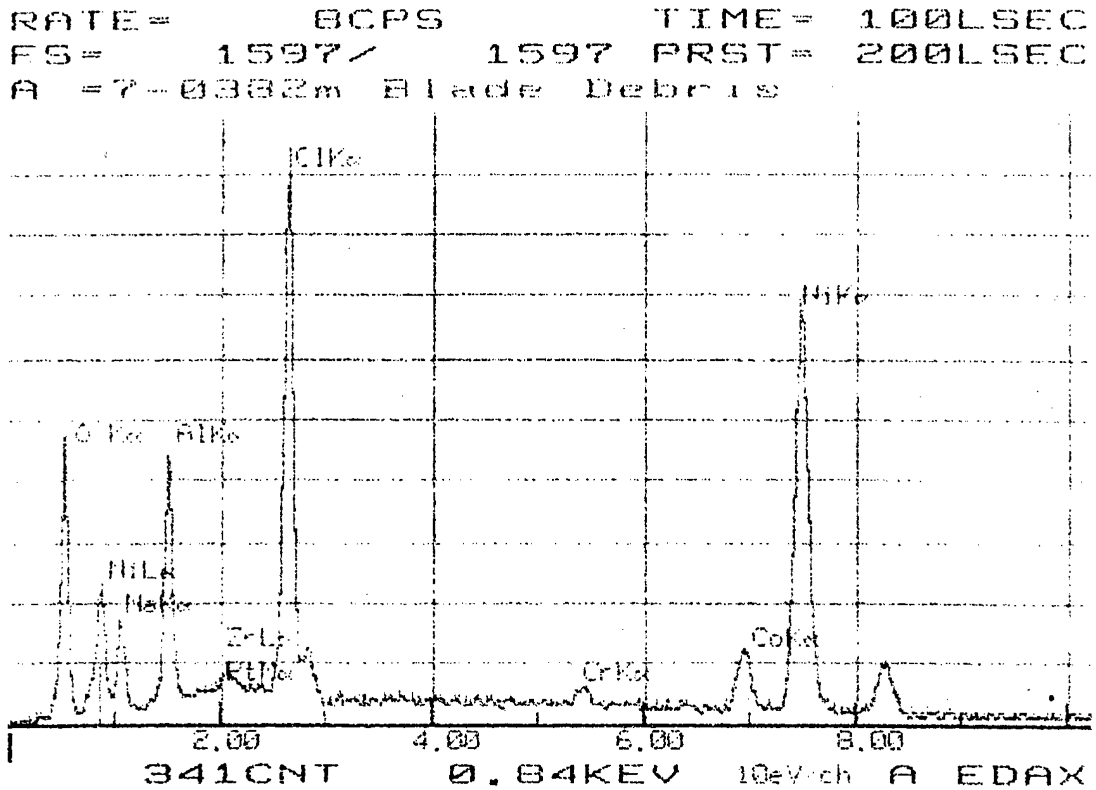


Figure 9. Energy Dispersive Spectrum of green residue on Ultramet blade after salt spray testing.